Journal of Alloys and Compounds 503 (2010) 76–81

Contents lists available at ScienceDirect

Journal of Alloys and Compounds

journal homepage: www.elsevier.com/locate/jallcom

Review

Properties and microstructure of AlN prepared using alumina crucible and $MoSi_2$ heating element

Chih-Peng Lin [a,*], Ya-Min Hsieh [b], Chih-Hung Chu [c]

[a] Department of Leisure and Recreation Management, Diwan College of Management, Tainan 721, Taiwan
[b] General Education Center, Diwan College of Management, Tainan 721, Taiwan
[c] Department of Resources Engineering, National Cheng Kung University, Tainan 701, Taiwan

ARTICLE INFO

Article history:
Received 2 February 2010
Received in revised form 30 April 2010
Accepted 30 April 2010
Available online 7 May 2010

Keywords:
Aluminum nitride
Critical temperature
Thermal conductivity
Dielectric
Hardness

ABSTRACT

Thermal conductivity, electrical, and mechanical properties of aluminum nitride (AlN) ceramics doped with Y_2O_3 and CaO and using a conventional $MoSi_2$ heating element furnace were investigated. Relative densities of over 98% of the theoretical values show that the critical sintering temperature for AlN densification may be as low as 1650 °C. An AlN ceramic with 1 wt.% Y_2O_3 and 1 wt.% CaO fired at 1700 °C for 3 h has a thermal conductivity of 110 W m^{-1} K^{-1} and a Vicker's hardness of 1053 kg mm^{-2}. Its dielectric constant and loss factor are 9.97 and 1.1×10^{-3} at 1 MHz, respectively. Microprobe observations of the test samples reveal that the thermal conductivities are related to the secondary phase composition and elemental distribution at grain boundaries and the oxygen content of sintered AlN.

Contents

1. Introduction

Aluminum nitride is a relatively new packaging material that evolved during the 1980s [1–4]. It is an alternative to BeO without the toxicity concerns. In general, its electrical properties (dielectric constant, loss tangent, resistivity, and dielectric strength) and mechanical properties (bending strength, hardness, toughness, and thermal expansion) are comparable to those of alumina and beryllia (BeO). However, AlN has low sinterability because it is a covalent material with the wurtzite-type structure [5]. Several studies on AlN ceramics have focused on the reduction of sintering temperature for densification. Arinaga et al. [6] reported that the lowest eutectic temperatures in AlN–CaO–Al_2O_3 and AlN–Y_2O_3–Al_2O_3 systems are nearly 1290 °C and 1686 °C, respectively. Troczynski and Nicholson [7] obtained dense AlN using 9 wt.% additives of CaO, Y_2O_3, SiO_2, La_2O_3, and CeO_2 at 1600 °C. Results of thermal conductivity and Vicker's hardness for the liquid-phase-rich material were 130 W m^{-1} K^{-1} and 11 GPa, respectively.

Recently, He et al. [8] prepared dense AlN ceramics by spark plasma sintering (SPS) at a low sintering temperature of 1700 °C for 10 min with Sm_2O_3 as the sintering additive. Yao et al. [9] reported that the thermal conductivity of AlN ceramics doped with 3 wt.%

* Corresponding author. Tel.: +886 6 5718888; fax: +886 6 5718464.
E-mail address: ftirlin@gmail.com (C.-P. Lin).

0925-8388/$ – see front matter.
doi:10.1016/j.jallcom.2010.04.232

Table 1
Chemical composition of the starting materials.

Denotation	Additive composition		
	AlN (wt.%)	Y_2O_3 (wt.%)	CaO (wt.%)
YC11	98	1	1
YC12	97	1	2
YC31	96	3	1

Er_2O_3 is 106 W m^{-1} K^{-1}, which is a higher than those of AlN ceramics doped with 2 wt.% Y_2O_3. Additionally, Lee et al. [10] showed that AlN with 3 wt.% CaF_2 and 1.5 wt.% Al_2O_3 heat treated in a nitrogen atmosphere and a reducing atmosphere had thermal conductivities of 200 W m^{-1} K^{-1} and 193.4 W m^{-1} K^{-1}, respectively. Our laboratory has shown that the atomic weight of the rare-earth element may greatly affect the apparent density of a sintered AlN specimen. The lighter atomic species of yttrium (Y) renders a faster diffusion rate removing pores at the grain boundaries [11].

The primary objective of this work is to study the sintering of AlN doped with Y_2O_3 and CaO using our newly developed sintering technique [12]. The present study is a continuation of our work on the relationship between processing, microstructures, and properties of AlN ceramics sintered at temperatures of 1600 °C, 1650 °C, and 1700 °C with a 3 h soaking time using an alumina (Al_2O_3) crucible in a box-type furnace equipped with a $MoSi_2$ heating element in a conventional flow of nitrogen atmosphere.

2. Experimental procedures

AlN powder with a specific surface area of 1.6 m^2 g^{-1}, a particle size (D_{50}) of 0.83 μm, and an oxygen impurity content of 2.2 wt.% was used as the starting powder. Y_2O_3 powder (purity 99.9%, Alfa Aesar, 99.9%) was incorporated as the sintering additive. CaO additive was added as $CaCO_3$ (purity 99.8%, J.T. Baker). The composition of AlN powder is described in Table 1. AlN powders and sintering additives Y_2O_3 and CaO were mixed by vibration milling for 6 h using ethanol as the mixing medium. After being dried and passed through a 100-mesh sieve, the granulated powders were uniaxially pressed at 40 MPa in a steel die to make pellets (16.5 mm in diameter and 2 mm in thickness). The pellets were then cold isostatically pressed (ClPed) under 98 MPa and dewaxed at 550 °C for 1 h.

The experimental arrangement of procedure for sintering of compacts was employed by our newly developed sintering technique [12]. The pellets, which were embedded in a boron nitride (AVOCADO, 99%) powder bed, were sandwiched by BN disc that was placed in an Al_2O_3 crucible (SSA-S, 280 cm^3) completely enveloped by a carbon black (Alfa Aesar, 99.9%) powder bed. Then, the samples were sintered at 1600 °C, 1650 °C, and 1700 °C for 3 h, respectively, in a $MoSi_2$ heating furnace with a conventional flow of nitrogen atmosphere (Yunshan Co. Ltd. purity 95%).

After the samples were heated, their apparent density was measured using the Archimedes method. The crystalline phases in each specimen were identified using X-ray diffraction (XRD) with Cu Kα radiation (Siemens D5000) at 40 KV and 40 mA. The lattice parameters of each sample were obtained by scanning from 20° to 80° with a step size of 0.02° 2θ/s and a sampling time of 8 s/step using XRD with Cu Kα radiation. The oxygen content of each specimen was measured using an N/O analyzer (LECO, TC-300). Microstructure and chemical elements were observed by a scanning electron microscope (SEM) and back-scattered electron imagery (BSI, Hitachi S-3000N). The thermal conductivity at room temperature was determined from thermal diffusivity. Heat capacity was measured using a laser flash technique (Laser Flash LFA-447, ASTM E1461) and bulk density. Both surfaces were painted with silver paint as electrical contacts. The dielectric constant (ε) and loss factor ($\tan\delta$) of the samples were measured using an LCR meter (Agilent 4284A) at 1–1000 kHz, 1 V, and room temperature. The Vicker's hardness of polished samples was measured using a Vicker's hardness tester (Akashi AVK-C21 Hardness tester) with a load of 10 kg at the diamond tip.

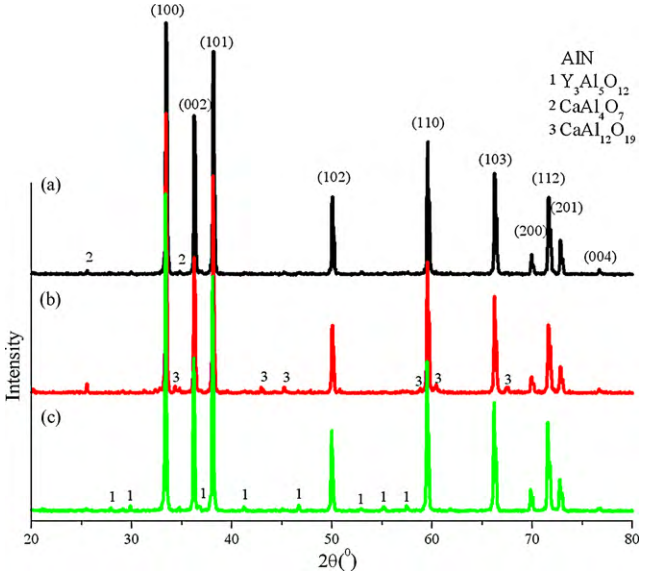

Fig. 1. X-ray diffraction profiles of (a) specimen YC11 (Y_2O_3 and CaO at 1 wt.% and 1 wt.%, respectively), (b) specimen YC12 (Y_2O_3 and CaO at 1 wt.% and 2 wt.%, respectively), and (c) specimen YC31 (Y_2O_3 and CaO at 3 wt.% and 1 wt.%, respectively) sintered at 1650 °C for 3 h.

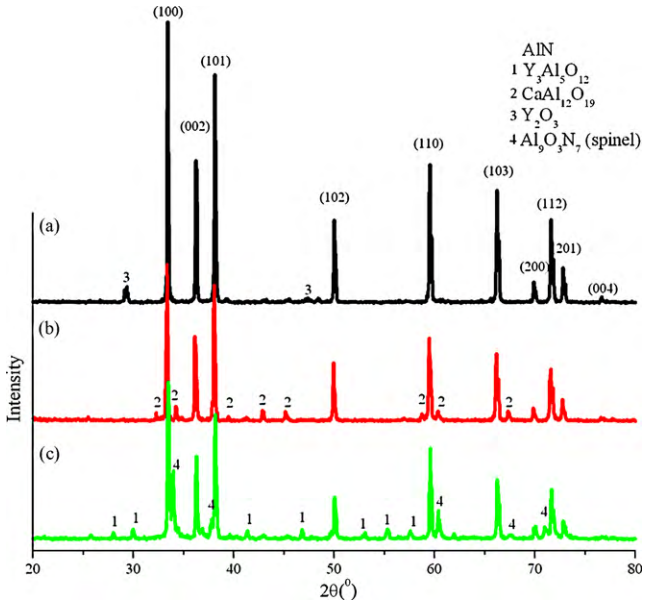

Fig. 2. X-ray diffraction profiles of (a) specimen YC11, (b) specimen YC12, and (c) specimen YC31 sintered at 1700 °C for 3 h.

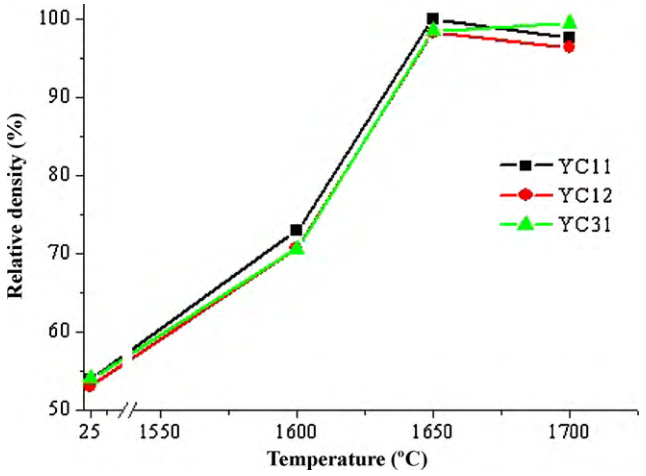

Fig. 3. Relative density of AlN specimens fired at various sintering temperature for 3 h.

Table 2
Density, oxygen content, lattice constant c, and thermal conductivities of samples sintered at 1650 °C and 1700 °C for 3 h.

Specimen	Temperature (°C)	Density (%)	Oxygen[a] content (wt.%)	O/N ratio[a]	Lattice constant *c* (Å)	Thermal conductivity ($W m^{-1} K^{-1}$)
YC11	1650	99.9	3.165	0.090	4.9755 (0.0003)	83.1
YC11	1700	97.6	n.a.	n.a.	4.9791 (0.0003)	110.0
YC12	1650	98.3	3.470	0.082	4.9763 (0.0003)	69.4
YC12	1700	96.4	3.573	0.104	4.9763 (0.0006)	82.0
YC31	1650	98.4	2.950	0.075	4.9780 (0.0004)	65.4
YC31	1700	99.4	3.098	0.076	4.9769 (0.0008)	n.a.[b]

[a] Determined using N/O analyzer.
[b] Not measured due to the formation of the AlON spinel phase with low thermal conductivity.

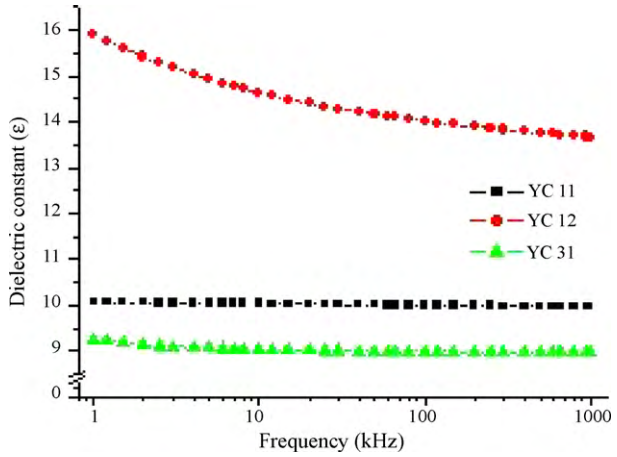

Fig. 4. Dielectric constant of AlN specimens with various amounts of Y_2O_3 and CaO sintered at 1700 °C for 3 h.

3. Results and discussion

3.1. Phase compositions of sintered AlN

The X-ray diffraction spectra of AlN samples with various amounts of Y_2O_3 and CaO content sintered at temperatures of 1650 °C and 1700 °C for 3 h are shown in Figs. 1 and 2, respectively. It can be seen that the AlN crystalline phase is the predominant phase in each specimen. For the specimen YC11, which had the lowest amount of Y_2O_3 and CaO and was fired at 1650 °C, trace amounts of $CaAl_4O_7$ and $Y_3A1_5O_{12}$ were found as secondary phases, which transformed into Y_2O_3 at 1700 °C. The specimen YC12 (with 1 wt.% Y_2O_3 and 2 wt.% CaO, fired at 1650 °C) exhibited a low amount of $CaAl_{12}O_{19}$ and a trace amount of $CaAl_4O_7$ as secondary phases. At a temperature of 1700 °C, the minor phase $CaAl_{12}O_{19}$ increased and the low eutectic phase $CaAl_4O_7$ disappeared. The X-ray profile of specimen YC31 (with 3 wt.% Y_2O_3 and 1 wt.% CaO), shows $Y_3A1_5O_{12}$ ($3Y_2O_3:5Al_2O_3$) as the minor phase for temperatures of 1650 °C and 1700 °C. In addition, at a temperature of 1700 °C, the appearance of $Al_9O_3N_7$ (a like spinel phase) was observed.

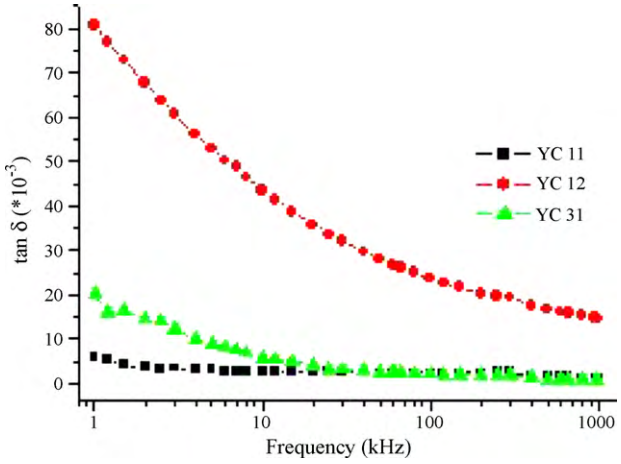

Fig. 5. Dielectric loss (tan δ) of AlN specimens with various amounts of Y_2O_3 and CaO sintered at 1700 °C for 3 h.

Table 3
Dielectric constant (ε) and loss (tan δ) of specimens with additives of Y_2O_3 and CaO sintered at 1650 °C for 3 h.

Specimen	10 kHz		100 kHz		1000 kHz	
	ε	tan δ (10^{-3})	ε	tan δ (10^{-3})	ε	tan δ (10^{-3})
YC11	10.24	0.47	10.23	0.78	10.22	0.08
YC12	10.64	0.10	10.62	0.77	10.62	0.02
YC31	10.68	17.0	10.64	27.9	10.61	13.1

3.2. Densification of sintered AlN

The relative densities of AlN specimens fired at various temperatures for 3 h are shown in Fig. 3. Densification of AlN specimens increased when the temperature was increased from room temperature to 1650 °C. The temperature at which the highest densities (about 98% of theoretical values) were obtained was 1650 °C for the series of test runs. A higher sintering temperature of 1700 °C did not show to be beneficial for augmenting the densification of AlN specimens. Figs. 1 and 2 show that the lower eutectic $CaAl_4O_7$ phase was eliminated by firing at a higher temperature of 1700 °C. According to previous works [13–16], the addition of lithium (Li) may quickly reduce the sintering temperature to below 1600 °C and 1550 °C, respectively.

3.3. Oxygen concentration and thermal conductivities

Generally speaking, the thermal conductivity is influenced by several factors, which may be divided into primary and secondary

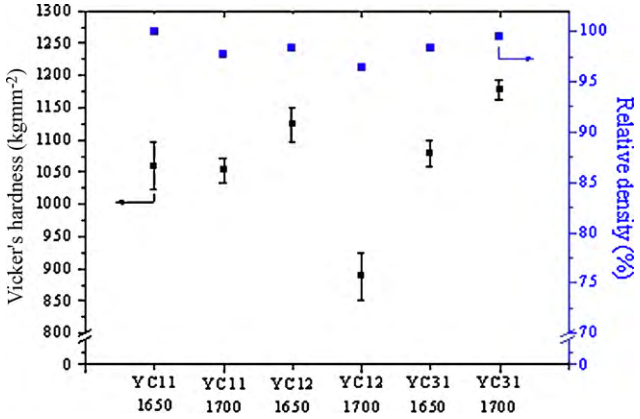

Fig. 6. Vicker's hardness of AlN samples with additives of Y_2O_3 and CaO sintered at 1650 °C and 1700 °C for 3 h.

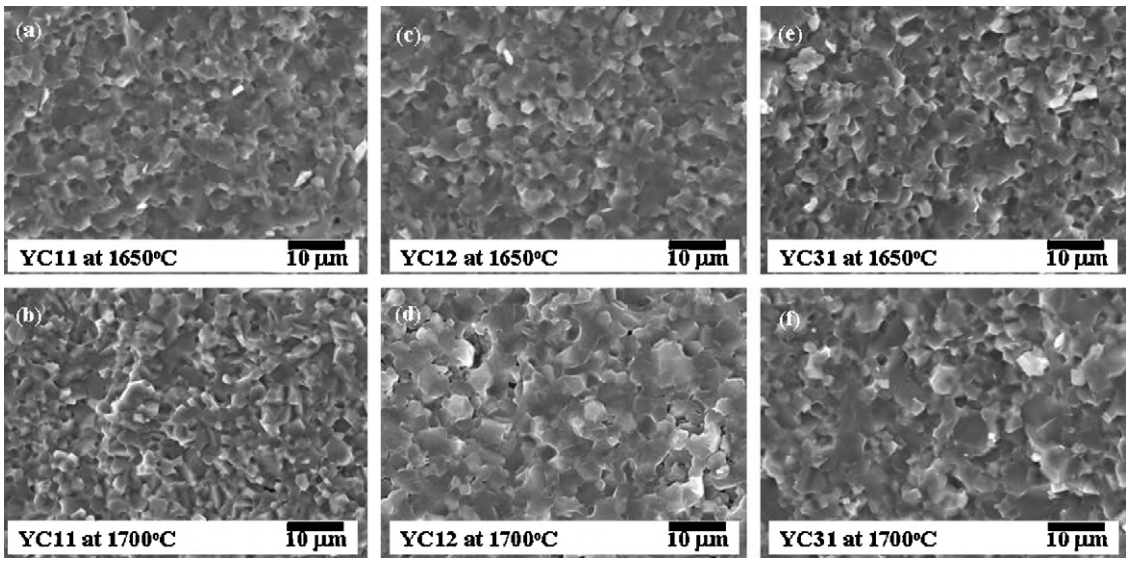

Fig. 7. SEM fractographs of sample YC11 sintered at (a) 1650 °C and (b) 1700 °C; those of sample YC12 sintered at (c) 1650 °C; and (d) 1700 °C; and those of sample YC31 sintered at (e) 1650 °C and (f) 1700 °C.

sources. The primary factors are material-dependent, such as the oxygen content (total and lattice dissolved), the microstructure, and lattice defects. Secondary factors include sintering conditions, sintering temperature, time, and sintering additives [17].

The oxygen content in the starting powder used in this study (i.e., 2.2 wt.%) is much higher than that of powders made with Tokuyama Soda and ART. A box-type furnace that does not accurately control the reduction atmosphere was employed. As a result, a higher total oxygen content within sintered AlN should be obtained during heat treatment, which has a detrimental effect on the properties of specimens.

Table 2 summarizes the thermal conductivities for three samples separately treated at two temperature levels, 1650 °C and 1700 °C, for 3 h. The results show that (a) specimen YC11 (1 wt.% Y_2O_3 and 1 wt.% CaO) sintered at 1700 °C has the highest thermal conductivity of 110 W m^{-1} K^{-1}; (b) specimen YC11 sintered at 1650 °C and specimen YC12 (1 wt.% Y_2O_3 and 2 wt.% CaO) sintered at 1700 °C have thermal conductivities of 83.1 W m^{-1} K^{-1} and 82.0 W m^{-1} K^{-1}, respectively. Table 2 shows that the *c*-axis in specimen YC11 sintered at 1700 °C is the highest so that the low probability of aluminum vacancy formed due to oxygen atom is substituted for nitrogen site.

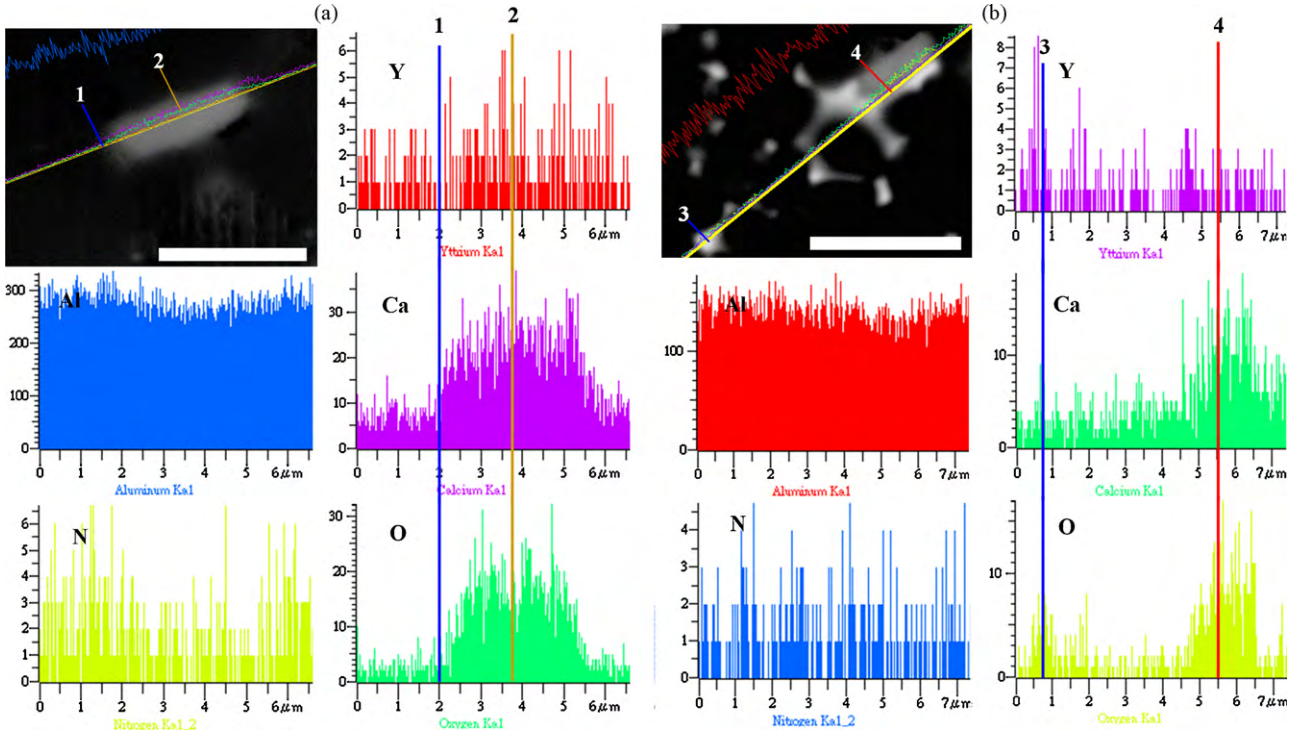

Fig. 8. Chemical element characterization of the morphology of secondary phases in the sintered AlN observed by line scanning of SEM. (bars = 3 μm) Location (1) shows AlN matrix and location (2) shows Ca–Al–O compound in (a); Location (3) shows Y–Al–O and location (4) shows Ca–Al–O compounds in (b).

Specimen YC12 sintered at 1650 °C and specimen YC31 (3 wt.% Y_2O_3 and 1 wt.% CaO) sintered at 1650 °C have the lowest thermal conductivities of 69.4 W m^{-1} K^{-1} and 65.4 W m^{-1} K^{-1}, respectively. Specimens YC12 and YC31 also have the lower densities, 98.3% and 98.4%, respectively, even though they were heated at a temperature of 1650 °C. The thermal conductivities vary with the ratio of Y_2O_3 and CaO; this generates various microstructures, giving secondary as well as minor phases.

3.4. Electrical properties

Table 3 shows the dielectric constant (ε) and loss factor ($\tan\delta$) of AlN specimens with various amounts of Y_2O_3 and CaO sintered at 1650 °C for 3 h. For a given relative density, the dielectric constant is similar for each specimen. Additionally, the loss factors ($\tan\delta$) of specimens YC11 and YC12 were calculated as 0.02 and 0.03×10^{-3}, respectively, for a frequency of 1 MHz, which are lower than that of specimen YC31 with 3 wt.% Y_2O_3 and 1 wt.% CaO addition.

As indicated in Figs. 4 and 5, the dielectric constant (ε) and loss factor ($\tan\delta$) of sintered AlN decrease with increasing frequency. The ε and $\tan\delta$ values at 1 MHz of specimen YC12 are 13.7 and 14.6×10^{-3}, respectively, which are higher than those of specimens YC11 and YC31. Fig. 7(d) shows that the grain size of sample YC12 (with 2 wt.% CaO added and fired at 1700 °C) is distinctly larger than those of other samples. In this study, the values of dielectric constant at 1 MHz are a little higher than those reported in [18,19], which are 9 and 9.4, respectively, (the dielectric constant for commercial AlN ceramics is between 8.6 and 9.0 [20]), whereas the values of $\tan\delta$ are a little lower than those reported in Refs. [19,23], which are 2 and 1.4×10^{-3}, respectively.

3.5. Mechanical properties

The Vicker's hardness and relative density of samples doped with Y_2O_3 and CaO and sintered at 1650 °C and 1700 °C for 3 h are shown in Fig. 6. The hardness of specimen YC12 (with 1 wt.% Y_2O_3 and 2 wt.% CaO) decreased from 1124 kg mm^{-2} at 1650 °C to 888 kg mm^{-2} at 1700 °C, which is be related to the increasing porosity of samples and grain growth on the microstructures. Cai et al. [19] reported that the hardness of AlN sample doped with mere CaO and fired at 1800 °C for 1 h was 1210 kg mm^{-2} with the load of 10 kg. The Vicker's hardness of specimen YC31 increased from 1079 kg mm^{-2} to 1178 kg mm^{-2} for sintering temperatures of 1650 °C and 1700 °C, respectively.

Table 4 summarizes the thermal, dielectric, and hardness properties of sintered AlN obtained in this study compared to those obtained in previous reports [13,19,21–25]. An AlN product with a slightly high dielectric constant, an intermediate thermal conductivity, and a suitable value of hardness can be obtained by employing the proposed sintering procedure.

3.6. Microstructures by SEM and microprobe analyses for minor phases

Fig. 7 shows the SEM photographs of the samples. The fracture surfaces of specimen YC11 (with the lowest amount of Y_2O_3 and CaO) and YC31 (with the highest amount of Y_2O_3 at 3 wt.% and CaO at 1 wt.%) sintered at 1650 °C and 1700 °C for 3 h had no residual porosity and exhibited similar homogenous grains. The results are fully consistent with the measured values for density. A comparison of Fig. 7(c) and (d) shows that specimen YC12 (with 1 wt.% Y_2O_3 and 2 wt.% CaO sintered at 1700 °C), had a lower density. Facts of grain boundaries may be noted to have more rounded features.

Fig. 8 shows that the chemical element analyses of the phases as revealed by SEM microprobe, Fig. 8(a) shows the analysis of the major phase of Ca–Al–O; whereas Fig. 8 (b) shows that of dual

Table 4
Phases and properties of sintered AlN.

Sintering conditions			Additives	Properties			Ref.
Kind of crucible	Powder bed	Setting and sintering temperature		Thermal conductivity (W m^{-1} K^{-1})	Dielectric constant and $\tan\delta \times 10^{-3}$ (1 MHz)	Vicker's hardness (kg mm^{-2})	
Al_2O_3	BN, carbon black	1700 °C for 3 h, $MoSi_2$ heating furnace in N_2 gas.	Y_2O_3–CaO	110	9.97 1.1	1053	This study
AlN		1600 °C for 10 h, graphite heating element in N_2 gas.	$YLiO_2$	176	n.a. n.a.	n.a.	[13]
		1600 °C for 1 min, double spark plasma sintering cycle in vacuum.	Sm_2O_3	90	9.0 n.a.	n.a.	[18]
	AlN	1800 °C for 1 h	CaO	n.a.	9.4 2	1210[a]	[19]
AlN plates		1750 °C for 1 h, graphite heating element in 0.1–0.2 MPa N_2 gas.	Y_2O_3	n.a.	n.a. n.a.	1091[b]	[21]
		1900 °C for 2 h, in flowing N_2 gas .	Y_2O_3	>160	8.5 <2 (14 GHz)	n.a.	[22]
BN		1750 °C for 1 h, graphite heating element in N_2 gas.	$CaCN_2$	n.a.	n.a. 1.4	n.a.	[23]
Graphite	AlN	1600 °C for 1 h, in N_2 gas.	Y_2O_3–CaO–La_2O_3–CeO_2–SiO_2	130	n.a. n.a.	1121[c]	[7]
Sagger		1800 °C for 2 h, graphite heating element in N_2 gas.	Y_2O_3–TiO_2	169	8.5 3.5 (10 GHz)	n.a.	[24]

[a] The hardness HV was evaluated by using a Vickers diamond at a load of 10 kg.
[b] The hardness HV at 2 kg load was measured using the Vickers indentation method [25].
[c] The hardness HV obtained by Vickers indentation with a 3 kg load.

phases of Y–Al–O and Ca–Al–O. It is noted that the additive Y_2O_3 can promote grain boundary diffusion [12]. It gives the optimum distribution of grain boundary phases located at AlN grains, leading to higher AlN thermal conductivity.

4. Conclusion

It is feasible to employ an alumina crucible and a conventional $MoSi_2$ heating element furnace to obtain dense AlN ceramic bodies; seemingly, we have shown that the use of high-purity N_2 atmosphere furnaces may not necessary. The AlN sample with a composition of 1 wt.% Y_2O_3 and 1 wt.% CaO treated at 1700 °C for 3 h had a thermal conductivity of 110 $W m^{-1} K^{-1}$, a dielectric constant of 9.97 (1 MHz), a loss factor of 1.1×10^{-3} (1 MHz), and a hardness of 1053 $kg mm^{-2}$. Its thermal conductivity is related to the secondary phase composition and elemental distribution at grain boundaries and the oxygen content of sintered AlN.

Acknowledgements

The authors would like to thank Prof. C.S. Huang for CIPed operation, Prof. S.L. Chung for N/O analysis, Prof. C.Y. Huang for measurements of dielectric properties and lattice parameter calculations, Prof. J.L. Huang for measurements of mechanical properties and Yonyu Applied Technology Material Co., Ltd. for measurements of thermal conductivity. We sincerely wish to thank Dr. H.S. Liu for discussion and improving the English writing.

References

[1] D. Wilson, H.D. Stenzenberger, P.M. Hergenrother, Polyimides, Chapman and Hall, New York, 1990.
[2] S.L. Rosen, Fundamental Principles of Polymeric Materials, Wiley, New York, 1993.
[3] W.F. Smith, Principles of Materials Science and Engineering:, Second Edition, McGraw-Hill, New York, 1990.
[4] R.D. Rossi, Polyimides, reprint from Engineering Materials Handbook, in: Adhesives and Sealants, vol. 3, ASM International, Cleveland, Ohio, 1991.
[5] Y. Kurokawa, K. Utsumi, H. Takamizawa, J. Am. Ceram. Soc. 71 (1988) 588–594.
[6] S. Arinaga, K. Shinozaki, N. Mizutani, in Proceedings of Annual Meeting of the Ceramics Society of Japan (Ceramics Society of Japan, Nagoya, Japan, 1994), p. 349.
[7] T.B. Troczynski, P.S. Nicholson, J. Am. Ceram. Soc. 72 (1989) 1488–1491.
[8] X. He, F. Ye, H. Zhang, L. Liu, J. Alloys Compd. 482 (2009) 345–348.
[9] Y. Yao, L. Wang, C. Li, X. Jiang, T. Qiu, Rare Met. 28 (2009) 596–599.
[10] H.K. Lee, D.K. Kim, Mod. Phys. Lett. B 23 (2009) 3869–3876.
[11] C.H. Chu, Y.H. Shen, C.P. Lin, S.B. Wen, J. Kor. Phys. Soc. 52 (2008) 1545–1549.
[12] C.H. Chu, C.P. Lin, S.B. Wen, Y.H. Shen, Ceram. Int. 35 (2009) 3455–3461.
[13] K. Watari, H.J. Hwang, M. Toriyama, S. Kanzaki, J. Am. Ceram. Soc. 79 (1996) 1979–1981.
[14] K. Watari, M.C. Valecillos, M.E. Brito, M. Toriyama, S. Kanzaki, J. Am. Ceram. Soc. 79 (1996) 3103–3108.
[15] K. Watari, H.J. Hwang, M. Toriyama, S. Kanzaki, J. Mater. Res. 14 (1999) 1409–1417.
[16] Y.C. Liu, Y. Wu, H.P. Zhou, Mater. Lett. 35 (1998) 232–235.
[17] A.M. Hundere, M.A. Einarsrud, J. Eur. Ceram. Soc. 17 (1997) 873–878.
[18] K.A. Khor, L.G. Yu, Y. Murakoshi, J. Eur. Ceram. Soc. 25 (2005) 1057–1065.
[19] K.F. Cai, D.S. McLachlan, Mater. Res. Bull. 37 (2002) 575–581.
[20] L.M. Sheppard, Am. Ceram. Soc. Bull. 69 (1990) 1801–1812.
[21] S. Burkhardt, R. Riedel, G. Müller, J. Eur. Ceram. Soc. 17 (1997) 3–12.
[22] S. Kume, M. Yasuoka, S.K. Lee, A. Kan, H. Ogawa, K. Watari, J. Eur. Ceram. Soc. 27 (2007) 2967–2971.
[23] M.C. Wang, C.C. Yang, N.C. Wu, Mater. Sci. Eng. A343 (2003) 97–106.
[24] M. Kasori, F. Ueno, A. Tsuge, J. Am. Ceram. Soc. 77 (1994) 1991–2000.
[25] G.R. Anstis, P. Chantikul, B.R. Lawn, D.B.A. Marshall, J. Am. Ceram. Soc. 64 (1981) 533–538.